

# Synthesis, Structures, and Magnetic Properties of Three Fluoride-Bridged Lanthanide Compounds: Effect of Bridging Fluoride Ions on Magnetic Behaviors

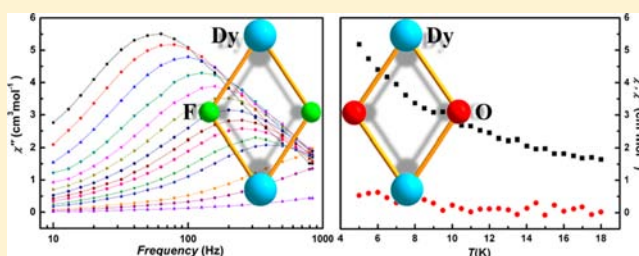
Qi Zhou,<sup>†</sup> Fen Yang,<sup>†</sup> Dan Liu,<sup>‡</sup> Yu Peng,<sup>†</sup> Guanghua Li,<sup>†</sup> Zhan Shi,<sup>\*,†</sup> and Shouhua Feng<sup>†</sup>

<sup>†</sup>State Key Laboratory of Inorganic Synthesis & Preparative Chemistry, College of Chemistry, Jilin University, Changchun 130012, People's Republic of China

<sup>‡</sup>State Key Laboratory of Rare Earth Resource Utilization, Changchun Institute of Applied Chemistry, Chinese Academy of Sciences, Changchun 130022, People's Republic of China

## S Supporting Information

**ABSTRACT:** A family of fluoride-bridged lanthanide compounds,  $[\text{Dy}^{\text{III}}\text{F}(\text{oda})(\text{H}_2\text{O})_3]$  (**1**, **oda** = oxidiacetate) and  $[\text{Ln}^{\text{III}}_2\text{F}_2(\text{oda})_2(\text{H}_2\text{O})_2]$  ( $\text{Ln} = \text{Tb}$ (**2**) and  $\text{Dy}$ (**3**)), was synthesized and characterized. To investigate the effects of bridging ligands on magnetic behaviors, two hydroxyl-bridged complexes of formulas  $[\text{Ln}^{\text{III}}_2(\text{OH})_2(\text{oda})_2(\text{H}_2\text{O})_4]$  ( $\text{Ln} = \text{Tb}$ (**4**) and  $\text{Dy}$ (**5**)) were also synthesized. Magnetic measurements show that the magnetic behaviors of the compounds are obviously distinct. Compounds **1**, **2**, and **3** show ferromagnetic interactions, while only antiferromagnetic interactions are observed in compounds **4** and **5**. Among these compounds, **1** and **3** show frequency-dependent ac-susceptibility indicative of slow magnetic relaxation. Because the structures of  $\text{Dy}_2$  cores are very similar in compounds **3** and **5**, it may be inferred that the differences of bridging ligands are mainly responsible for the distinct magnetic exchange interactions and relaxation dynamics.



Compounds **1** and **3** show frequency-dependent ac-susceptibility indicative of slow magnetic relaxation. Because the structures of  $\text{Dy}_2$  cores are very similar in compounds **3** and **5**, it may be inferred that the differences of bridging ligands are mainly responsible for the distinct magnetic exchange interactions and relaxation dynamics.

## INTRODUCTION

Since the dodecanuclear manganese cluster was obtained as the first single-molecule magnet (SMM),<sup>1</sup> SMMs and SCMs (single-chain magnets) have been of increasing interest, mainly because of their potential applications in high-density magnetic memories, quantum computing, and molecular spintronics.<sup>2</sup> Over the last two decades, a great number of transition-metal molecular magnets have been synthesized and their magnetic properties have been widely studied.<sup>3</sup> In recent years, lanthanide coordination compounds have attracted more and more attention in the field of molecular magnetism due to their significant magnetic anisotropy from the unquenched orbital angular momentum.<sup>4</sup> However, because of the efficient shielding of the unpaired electrons in the 4f orbitals, the weak exchange interactions between lanthanide ions have been a big stumbling block to the development of lanthanide-only molecular magnets. The way to overcome this obstacle is to select a suitable bridging ligand which can promote magnetic interactions between the lanthanide ions through the overlap of bridging ligand orbitals with the 4f orbitals of the Ln ions.<sup>5</sup> In addition, since the relaxation barrier is mainly attributable to the individual anisotropies of the metal ions in the lanthanide complexes, the bridging ligands will affect the magnetic relaxation behaviors through altering the nature or directions of the easy axes.<sup>6</sup> To date, only a few kinds of bridging ligands have been employed, including phenoxide,<sup>7</sup> carboxyl,<sup>8</sup> nitronyl nitroxide radical,<sup>9</sup> carbonate,<sup>10</sup> pyrazine,<sup>11</sup> hydroxyl,<sup>12</sup> oxalate,<sup>13</sup> and tetrathiafulvalene.<sup>14</sup> Not long ago, Long and colleagues successfully

synthesized  $\text{N}_2^{3-}$  radical-bridged dilanthanide complexes, which reveal exceptionally strong magnetic exchange interactions, giving rise to a new record SMM.<sup>15</sup> In order to investigate the effects of bridging ligands on magnetic behaviors, it is necessary and challenging to explore new bridging ligands.

Until now, the great majority of the ligands bridge lanthanide ions through N or O atoms. In comparison with the N or O bridging ligands, fluoride ions possess smaller ionic radius and larger electronegativity. In addition, they can bridge between metal ions in idiographic ways.<sup>16</sup> Therefore,  $\text{F}^-$  ions have been used to construct 3d and 3d–4f molecular magnets.<sup>17</sup> Surprisingly, fluoride-bridged lanthanide-based coordination compounds are very limited. Furthermore, the studies mainly focus on their structures and optical properties,<sup>18</sup> whereas their magnetic behaviors have largely been underexplored. To the best of our knowledge, the effects of bridging  $\text{F}^-$  ions on magnetic behaviors have never been discussed in the lanthanide coordination compounds.

In the present work, we obtained a family of fluoride-bridged lanthanide compounds, coordination compounds of formulas,  $[\text{Dy}^{\text{III}}\text{F}(\text{oda})(\text{H}_2\text{O})_3]$  (**1**, **oda** = oxidiacetate) and  $[\text{Ln}^{\text{III}}_2\text{F}_2(\text{oda})_2(\text{H}_2\text{O})_2]$  ( $\text{Ln} = \text{Tb}$ (**2**) and  $\text{Dy}$ (**3**)). To investigate the effect of  $\text{F}^-$  bridging ligands on the magnetic behaviors, two hydroxyl-bridged compounds of formulas  $[\text{Ln}^{\text{III}}_2(\text{OH})_2(\text{oda})_2(\text{H}_2\text{O})_4]$  ( $\text{Ln} = \text{Tb}$ (**4**) and  $\text{Dy}$ (**5**)) were also synthesized

Received: January 18, 2012

Published: July 2, 2012

Table 1. Crystallographic Data for 1–5

compound	1	2	3	4	5
formula	C <sub>4</sub> H <sub>10</sub> FO <sub>8</sub> Dy	C <sub>8</sub> H <sub>12</sub> F <sub>2</sub> O <sub>12</sub> Tb <sub>2</sub>	C <sub>8</sub> H <sub>12</sub> F <sub>2</sub> O <sub>12</sub> Dy <sub>2</sub>	C <sub>8</sub> H <sub>18</sub> O <sub>16</sub> Tb <sub>2</sub>	C <sub>8</sub> H <sub>18</sub> O <sub>16</sub> Dy <sub>2</sub>
fw (g mol <sup>-1</sup> )	367.62	656.02	663.18	688.06	695.22
cryst syst	monoclinic	monoclinic	monoclinic	monoclinic	triclinic
space grp	<i>P</i> <sub>2</sub> / <i>n</i>	<i>C</i> <sub>2</sub> / <i>m</i>	<i>C</i> <sub>2</sub> / <i>m</i>	<i>P</i> <sub>2</sub> / <i>c</i>	<i>P</i> -1
<i>a</i> (Å)	7.282(8)	9.281(6)	9.255(5)	10.865(4)	6.715(9)
<i>b</i> (Å)	7.084(7)	9.671(2)	9.673(1)	6.757(7)	10.713(3)
<i>c</i> (Å)	17.810(7)	9.032(1)	9.019(0)	11.314(3)	11.275(5)
$\alpha$ (deg)	90	90	90	90	84.20(3)
$\beta$ (deg)	100.45(9)	117.28(5)	117.14(4)	95.76(4)	88.72(3)
$\gamma$ (deg)	90	90	90	90	89.90(3)
<i>V</i> (Å <sup>3</sup> )	903.70(6)	720.55(7)	718.53(5)	826.55(4)	806.8(3)
<i>Z</i>	4	2	2	2	2
<i>F</i> (000)	692	608	612	648	652
<i>D</i> <sub>calcd</sub> (g cm <sup>-3</sup> )	2.702	3.024	3.065	2.765	2.862
<i>T</i> (K)	293	293	293	293	293
<i>R</i> <sub>1</sub> <sup>a</sup>	0.0369	0.0286	0.0195	0.0234	0.0238
<i>wR</i> <sub>2</sub> <sup>b</sup>	0.0896	0.0781	0.0436	0.0654	0.0629

$$^a R_1 = \frac{\sum |F_o| - |F_c|}{\sum |F_o|}; \quad ^b wR_2 = \frac{\{\sum [w(F_o^2 - F_c^2)^2] / \sum [w(F_o^2)]\}^{1/2}}{\sum [w(F_o^2)]^{1/2}}; \quad w = 1 / [\sigma^2(F_o)^2 + (0.0511P)^2 + 19.56P], \quad \text{where } P = [F_o^2 + 2|F_c|^2] / 3.$$

as a comparison. Oxydiacetate has been widely employed in lanthanide coordination compounds.<sup>19</sup> Interestingly, the differences of bridging ligands are mainly responsible for the distinct magnetic exchange interactions and relaxation dynamics observed. In compounds **1**, **2**, and **3**, ferromagnetic interactions were clearly observed, but antiferromagnetic interactions were observed between lanthanide ions in **4** and **5**. Furthermore, compounds **1** and **3** exhibit frequency-dependent on alternating-current magnetic susceptibilities, indicating slow magnetic relaxation, while no frequency-dependence of out-of-phase signals was observed in the others.

## EXPERIMENTAL SECTION

**Synthesis.** All reagents and solvents were commercially available and were used without further purification.

**[Dy<sup>III</sup>F(oda)(H<sub>2</sub>O)<sub>3</sub>] (1).** A mixture of Dy(NO<sub>3</sub>)<sub>3</sub>·6H<sub>2</sub>O (1 mmol, 0.455 g), H<sub>2</sub>oda (0.6 mmol, 0.153 g) and NaF (1 mmol, 0.042 g) in H<sub>2</sub>O (12 mL) was stirred for 30 min, followed by the addition of NaOH (2 mmol, 0.080 g). The resulting mixture was stirred for 15 min, then heated in a Teflon-lined steel bomb at 60 °C for 3 days. Colorless block-shaped crystals formed were collected in 57% yield (based on Dy). IR (KBr, cm<sup>-1</sup>): 3220(m), 2956(w), 1666(s), 1604 (s), 1428(s), 1317(m), 1122(s), 1056(m), 937(m), 800(w), 719(w), 616(w), 581(w). Elem. Anal. Calcd. (%) for C<sub>4</sub>H<sub>10</sub>DyFO<sub>8</sub>: C, 13.07; H, 2.74. Found: C, 13.31; H, 2.81.

**[Tb<sup>III</sup><sub>2</sub>F<sub>2</sub>(oda)<sub>2</sub>(H<sub>2</sub>O)<sub>2</sub>] (2).** This was prepared in a similar way to **1**, but using Tb(NO<sub>3</sub>)<sub>3</sub>·6H<sub>2</sub>O (1 mmol 0.453 g) instead of Gd(NO<sub>3</sub>)<sub>3</sub>·6H<sub>2</sub>O heated at 160 °C in 45% yield. IR (KBr, cm<sup>-1</sup>): 3401(m), 2938(w), 1589(s), 1431(s), 1310(s), 1128(s), 1055(w), 994(w), 727(m), 556(m). Elem. Anal. Calcd. (%) for C<sub>8</sub>H<sub>12</sub>F<sub>2</sub>O<sub>12</sub>Tb<sub>2</sub>: C, 14.65; H, 1.84. Found: C, 14.71; H, 1.88.

**[Dy<sup>III</sup><sub>2</sub>F<sub>2</sub>(oda)<sub>2</sub>(H<sub>2</sub>O)<sub>2</sub>] (3).** This was prepared in a similar way to **2**, using Dy(NO<sub>3</sub>)<sub>3</sub>·6H<sub>2</sub>O (1 mmol 0.455 g) instead of Tb(NO<sub>3</sub>)<sub>3</sub>·6H<sub>2</sub>O in 52% yield. IR (KBr, cm<sup>-1</sup>): 3409(m), 2940(w), 1590(s), 1433(s), 1306(s), 1122(s), 1051(w), 995(w), 728(m), 561(m). Elem. Anal. Calcd. (%) for C<sub>8</sub>H<sub>12</sub>Dy<sub>2</sub>F<sub>2</sub>O<sub>12</sub>: C, 14.49; H, 1.82. Found: C, 14.52; H, 1.86.

**[Tb<sup>III</sup><sub>2</sub>(OH)<sub>2</sub>(oda)<sub>2</sub>(H<sub>2</sub>O)<sub>4</sub>] (4).** This was prepared in a similar way to **2**, but using Na<sub>2</sub>CO<sub>3</sub> (1 mmol 0.106 g) instead of NaF in 20% yield. IR (KBr, cm<sup>-1</sup>): 3633(m), 3483(w), 3257(w), 3063(m), 1578(s), 1428(s), 1323(s), 1245(w), 1129(s), 1054(m), 933(w), 783(w), 453(w). Elem. Anal. Calcd. (%) for C<sub>8</sub>H<sub>18</sub>O<sub>16</sub>Tb<sub>2</sub>: C, 13.96; H, 2.63. Found: C, 14.02; H, 2.69.

**[Dy<sup>III</sup><sub>2</sub>(OH)<sub>2</sub>(oda)<sub>2</sub>(H<sub>2</sub>O)<sub>4</sub>] (5).** This was prepared in a similar way to **3**, but using Na<sub>2</sub>CO<sub>3</sub> (1 mmol 0.106 g) instead of NaF in 22% yield. IR (KBr, cm<sup>-1</sup>): 3639(m), 3488(w), 3253(w), 3064(m), 1587(s),

1432(s), 1317(s), 1245(w), 1126(s), 1056(m), 937(w), 775(w), 456(w). Elem. Anal. Calcd. (%) for C<sub>8</sub>H<sub>18</sub>Dy<sub>2</sub>O<sub>16</sub>: C, 13.82; H, 2.61. Found: C, 14.01; H, 2.68.

**Physical Measurements.** Elemental analyses of carbon and hydrogen were carried out on a Perkin-Elmer 240C elemental analyzer. IR spectra as KBr pellets were recorded with a Magna 750 FT-IR spectrophotometer using reflectance technique over the range of 4000–400 cm<sup>-1</sup>. X-ray powder diffraction (XRPD) patterns were taken on a Rigaku D/max 2550 X-ray Powder Diffractometer. X-ray photoelectron spectroscopy (XPS) data were collected on an ESCALAB 250 X-ray photoelectron spectroscopy, using Mg K $\alpha$  X-ray as the excitation source. All magnetization were obtained with a Quantum Design MPMS SQUID VSM magnetometer. The variable-temperature magnetic susceptibility was measured with an external magnetic field of 1000 Oe. Samples were restrained in eicosane to prevent torqueing. Pascal's constants were used to estimate the diamagnetic corrections, which were subtracted from the experimental susceptibilities to give the molar paramagnetic susceptibilities ( $\chi_M$ ).

**X-ray Crystallography.** Suitable single crystals for **1–5** were glued onto a glass fiber. Diffraction intensity data for **1–4** were collected with a Bruker Smart CCD diffractometer equipped with graphite-monochromated Mo-K $\alpha$  radiation ( $\lambda = 0.71073$  Å) at 293 K. Single-crystal structure determination of **5** was carried out on a Rigaku RAXIS-RAPID diffractometer equipped with graphite-monochromated Mo-K $\alpha$  radiation ( $\lambda = 0.71073$  Å) at 293 K. The intensity data sets were collected with the  $\omega$ -scan technique and reduced by CrystalClear software. The structures of the five compounds were solved by direct methods and refined with the full-matrix leastsquares technique using the program SHELXTL.<sup>20</sup> The location of metal atom was easily determined, and F, O, N, and C atoms were subsequently determined from the difference Fourier maps. Anisotropic thermal parameters were assigned to all non-hydrogen atoms. The disordered atoms were refined with constrained dimensions. The hydrogen atoms were set in calculated positions. The crystal data, data collection, and refinement parameters for complexes **1–5** are listed in Table 1, and selected bond lengths and angles for complexes **1–5** are listed in Table S2 of the Supporting Information. CCDC reference numbers for compounds **1–5** are 862413, 881773, 862414, 881775, and 862415, respectively.

## RESULTS AND DISCUSSION

**Crystal Structure.** *Compound 1.* crystallizes in the monoclinic space group *P*<sub>2</sub>/*n* and the structure is shown in Figure 1. A structural study of **1** shows it to be a 1D zigzag chain. The Dy<sup>III</sup> ion in the chain is coordinated by one oda<sup>2-</sup> ligand (O1, O2 and O4), two F<sup>-</sup> ions and three water molecules (O6, O7, and O8), leading to a coordination number of eight and a distorted dodecahedral

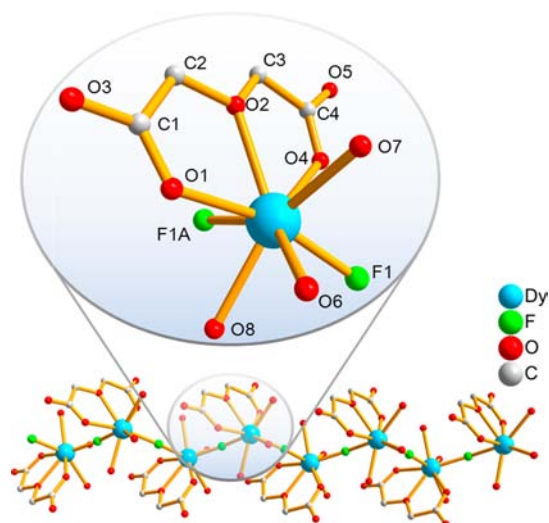


**Figure 1.** Asymmetric structure unit and polymeric structure of compound 1. Organic hydrogen atoms and minor disordered components have been omitted for clarity.

geometry. The fluorine ions linearly bridge neighboring dysprosium ions forming a 1D zigzag chain with a Dy–Dy distance of 4.39(7) Å and a Dy–F–Dy angle of 160.26(3)°. Similar linear fluoride bridges have been observed in fluorine-bridged transition-metal complexes.<sup>17e,21</sup> Intermolecular hydrogen bonding interactions appear between neighboring chains, thus, a 3D supramolecular structure is afforded. The shortest intermolecular Dy–Dy separation distance is 7.28(3) Å.

**Compounds 2 and 3.** These compounds are isomorphous and crystallize in the monoclinic space group  $C2/m$ . The structure of 3 will be described as a representative (Figure 2). The

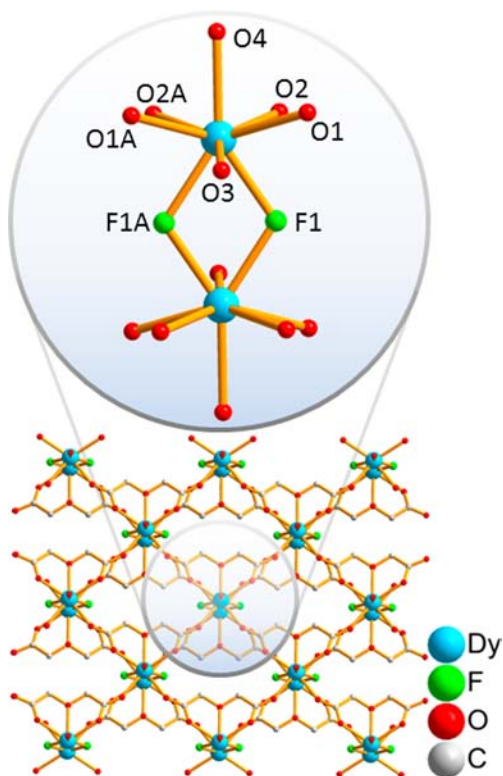


**Figure 2.** The Dy<sub>2</sub> cores and polymeric structure of compound 3. Organic hydrogen atoms and minor disordered components have been omitted for clarity.

centrosymmetric dinuclear core is composed of two eight-coordinate Dy<sup>III</sup> ions bridged by two F<sup>−</sup> ions, giving rise to a Dy<sub>2</sub>F<sub>2</sub> core with a Dy–Dy distance of 3.730(4) Å and a Dy–F–Dy angle of 112.39(3)°. Each Dy<sup>III</sup> ion of the dinuclear cores is coordinated by one oda<sup>2−</sup> ligand (O1, O3 and O1A), two F<sup>−</sup> ions and one water molecules (O4). The coordination sphere of the Dy<sup>III</sup> ion is completed by two oxygen atoms (O2 and O2A) of two bridging ada<sup>2−</sup> ligands forming a perfect two-dimensional rhombic grid of the dinuclear dysprosium complexes. The shortest intra network distance between the two Dy<sub>2</sub> cores is 6.69(4) Å. The 2D networks are further connected to form a 3D supramolecular structure by the hydrogen bondings between O4 from a coordinated water molecule and the oxygen atoms (O1 and O2) from the oda<sup>2−</sup> ligand located in the crystal lattice, making the shortest intermolecular Dy–Dy separation distance of 5.86(3) Å from different dinuclear units. The presence of F<sup>−</sup> ions was further confirmed by XPS (Figure S1 in the Supporting Information).

**Compound 4.** This compound crystallizes in the triclinic space group  $P2_1/c$ , and the structure is shown in Figure 3.

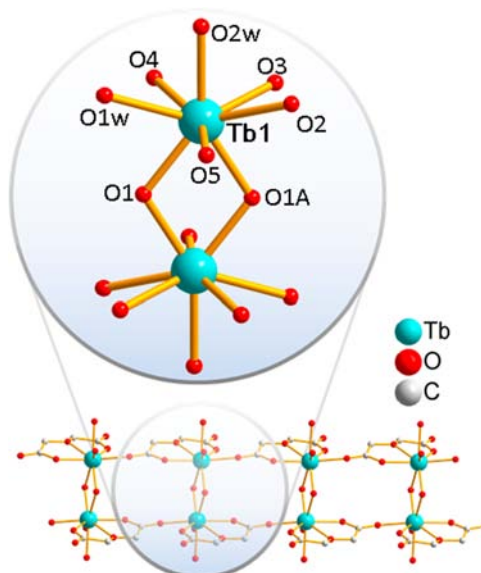


**Figure 3.** The Tb<sub>2</sub> cores and polymeric structure of compound 4. Organic hydrogen atoms and minor disordered components have been omitted for clarity.

The Ln<sub>2</sub> cores of complexes 4 and 3 are almost the same. The differences lie in that the bridging hydroxyls take the place of bridging F<sup>−</sup> ions. The Tb<sub>2</sub>(OH)<sub>2</sub> unit is also centrosymmetric with a Tb–Tb distance of 3.740(9) Å and a Tb–O–Tb angle of 110.90(6)°. The coordination sphere of the Tb<sup>III</sup> ion is made of eight oxygen atoms arising from two oda<sup>2−</sup> ligands (O2, O3, O4, and O5), two hydroxyls (O1 and O1A) and two water molecules (O1w and O2w). The Tb<sub>2</sub>(OH)<sub>2</sub> units are connected to form a 1D chain through oda<sup>2−</sup> ligands. The shortest intra-chain distance between the two Tb<sub>2</sub>(OH)<sub>2</sub> cores is 6.75(8) Å. A 3D supramolecular structure is formed by the hydrogen bonding interactions between neighboring chains, and the shortest intermolecular Tb–Tb separation distance is 6.43(3) Å from different Tb<sub>2</sub>(OH)<sub>2</sub> units.

**Compound 5.** This compound crystallizes in the triclinic space group  $P-1$ . The structure consists of two crystallographically unique, but structurally very similar dinuclear dysprosium units which are almost the same as the Tb<sub>2</sub>(OH)<sub>2</sub> core in compound 4. The differences lie in that the bridging hydroxyls

take the place of bridging  $F^-$  ions. In one dinuclear dysprosium unit, the Dy–Dy distance is 3.74(1) Å and the Dy–O–Dy angle is 110.90(6)°. In the other dinuclear dysprosium units, the Dy–Dy distance is 3.75(4) Å and the Dy–O–Dy angle is 113.34(9)°. The shortest intermolecular Dy–Dy separation distance is 6.14 (9) Å from different  $Dy_2(OH)_2$  units.

However, the structures of  $Ln_2$  cores are similar in compounds 2, 3, 4, and 5, although the bridging ions are different.  $Ln_2O_2$  cores are obtained in compounds 4 and 5. A number of lanthanide compounds which consist of similar  $Ln_2O_2$  cores have been reported, and their magnetic properties have been studied in-depth, such as  $[Dy_2(hmi)_2(NO_3)_2(MeOH)_2]$ ,  $[Dy_2(ovph)_2(NO_3)_2(H_2O)_2]$ ,  $[Tb_2(valdien)_2(NO_3)_2]$ , and  $[Gd_2(Hsabhea)_2(NO_3)_2]$ .<sup>22,7e,12e</sup> There are also a few precedents for fluoride-bridged lanthanide compounds, in which the structures of  $Ln_2F_2$  cores are close to those of compounds 2 and 3, such as  $[Yb_2F_2(OC_6H_4-2,6-tBu_2)_4(THF)_2]$ ,  $[Sm_2F_2\{(Me_3Si)_2C_5H_3\}_2]$ ,  $[Nd_2F_2\{(Me_3Si)_2C_5H_3\}_2]$ , and  $[Gd_2F_2\{(Me_3Si)_2C_5H_3\}_2]$ .<sup>18c,23</sup> But the investigations of their magnetic properties are very lacking. We tried to substitute for Dy ions in the reactions of compound 1, but unfortunately our efforts resulted in failure. All attempts to synthesize the  $Gd_2$  compound were also unsuccessful.

**Magnetic Properties.** Solid-state, variable-temperature dc magnetic susceptibility measured for the three compounds have been carried out in an applied magnetic field of 1000 Oe in the temperature range 2–300 K. The plots  $\chi T$  vs  $T$  are shown in Figure 4, where  $\chi$  is the molar magnetic susceptibility.

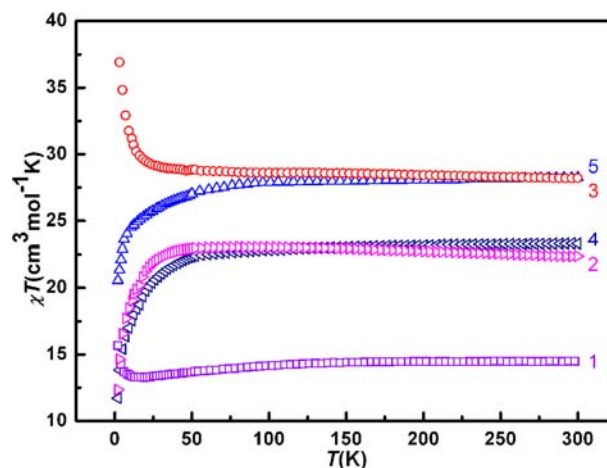


**Figure 4.** Temperature dependence of the  $\chi_M T$  product for compounds 1–5 at 1000 Oe.

For compound 1, the room temperature  $\chi T$  value is  $14.47 \text{ cm}^3 \text{K mol}^{-1}$ , in good agreement with that expected for an isolated  $Dy^{III}$  ion ( ${}^6H_{15/2}$ ,  $S = 5/2$ ,  $L = 5$ ,  $J = 15/2$ ,  $g = 4/3$ ,  $\chi T = 14.17 \text{ cm}^3 \text{K mol}^{-1}$ ). Upon decreasing the temperature, the  $\chi T$  product slightly decreases with the temperature to reach a minimum of  $13.25 \text{ cm}^3 \text{K mol}^{-1}$  at about 18 K, which is probably ascribed to antiferromagnetic exchange interactions and the progressive depopulation of excited Stark sublevels.<sup>24</sup> When the temperature is below 18 K, a clear increase can be observed and the  $\chi T$  reaches a maximum value of  $15.65 \text{ cm}^3 \text{K mol}^{-1}$  at 2 K.

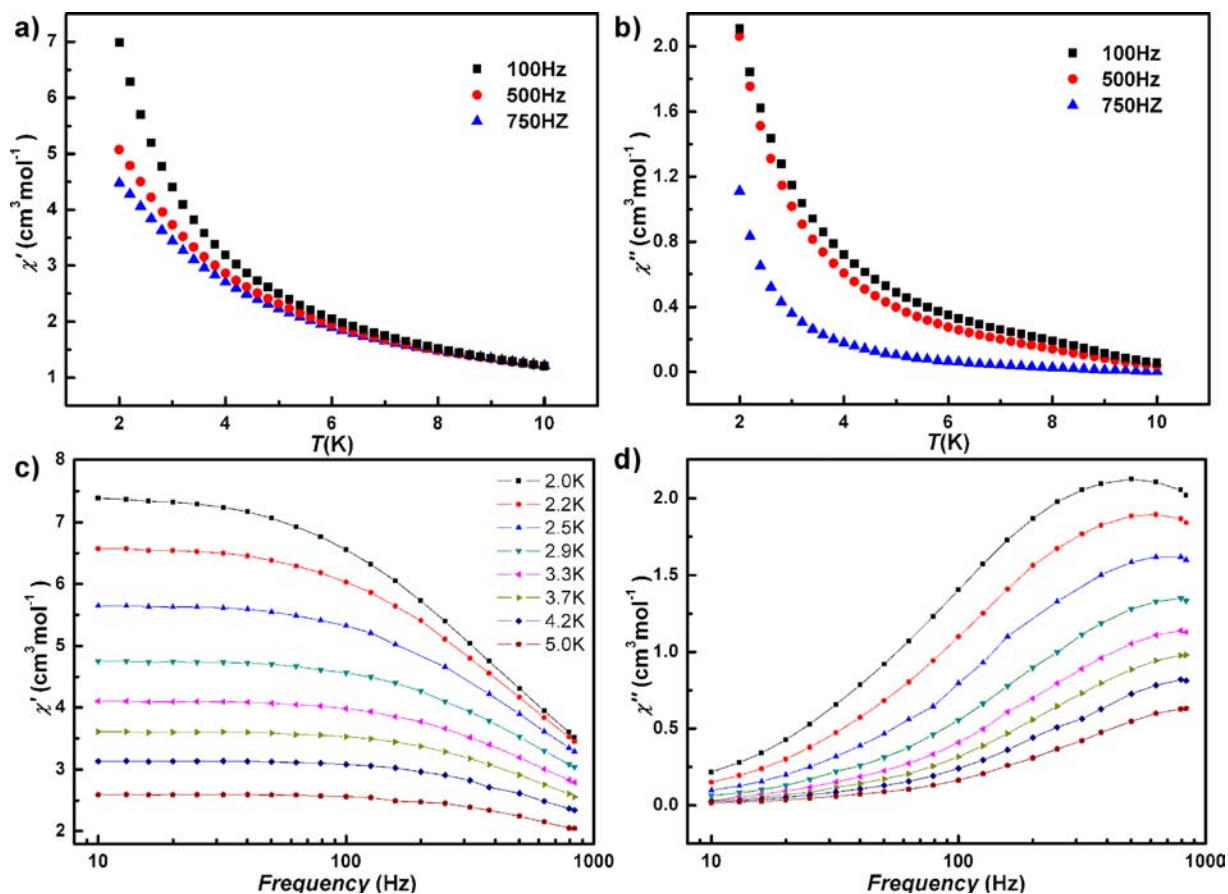


**Figure 5.** Temperature dependence of the in-phase (a) and out-of-phase (b) ac susceptibility and frequency dependence of in-phase (c) and out-of-phase (d) ac susceptibilities for compound 1 under zero dc field.

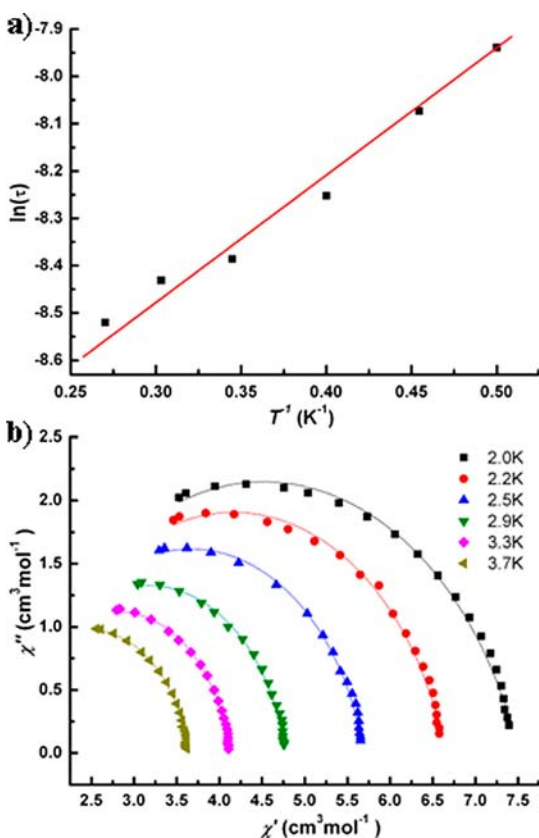


**Figure 6.** (a) Relaxation time,  $\ln(\tau)$ , versus  $T^{-1}$  plot for **1** under zero dc field. The solid line is fitted with Arrhenius law. (b) Cole–Cole plots measured in zero dc field for compound **1**. The solid lines are the best fits to the experiment data.

Such an increase indicates the presence of ferromagnetic interactions between the metal centers.<sup>25</sup>

For compound **2**, the  $\chi T$  value of  $22.48 \text{ cm}^3\text{K mol}^{-1}$  at 300 K corresponds exactly to the expected value of  $23.64 \text{ cm}^3\text{Kmol}^{-1}$

for two uncoupled  $\text{Tb}^{\text{III}}$  ions ( ${}^7\text{F}_6$ ,  $S = 3$ ,  $L = 3$ ,  $J = 6$ ,  $g = 3/2$ ,  $\chi T = 11.82 \text{ cm}^3\text{Kmol}^{-1}$ ). The  $\chi T$  product slightly increases with decreasing temperature to reach a maximum of  $23.04 \text{ cm}^3\text{Kmol}^{-1}$  at about 82 K, and then decreases sharply to a minimum value of  $12.34 \text{ cm}^3\text{Kmol}^{-1}$  at 2 K, which obviously suggests the presence of intramolecular ferromagnetic interactions between the metal centers. For compound **4**, the  $\chi T$  value of  $23.06 \text{ cm}^3\text{Kmol}^{-1}$  at 300 K is in close agreement with the expected value of  $23.64 \text{ cm}^3\text{Kmol}^{-1}$  for two uncoupled  $\text{Tb}^{\text{III}}$  ions. The  $\chi T$  product begins a slight decrease until 50 K, and then the rate of decrease becomes gradually larger. Finally, the  $\chi T$  product further decreases sharply and reaches a minimum of  $11.71 \text{ cm}^3\text{Kmol}^{-1}$  at 2 K. Thermal depopulation of the Stark sublevels is mainly responsible for the decrease. The weak antiferromagnetic interactions between the metal centers may also make some contribution.

For compound **3**, the  $\chi T$  value of  $28.21 \text{ cm}^3\text{K mol}^{-1}$  at 300 K corresponds exactly to the expected value of  $28.34 \text{ cm}^3\text{Kmol}^{-1}$  for two uncoupled  $\text{Dy}^{\text{III}}$  ions ( ${}^6\text{H}_{15/2}$ ,  $S = 5/2$ ,  $L = 5$ ,  $J = 15/2$ ,  $g = 4/3$ ,  $\chi T = 14.17 \text{ cm}^3\text{Kmol}^{-1}$ ). The  $\chi T$  product slightly increases with decreasing temperature until 50 K, and then increases sharply to a maximum value of  $36.64 \text{ cm}^3\text{K mol}^{-1}$  at 2 K, which obviously suggests the presence of intramolecular ferromagnetic interactions between the metal centers. For compound **5**, the  $\chi T$  value of  $28.24 \text{ cm}^3\text{Kmol}^{-1}$  at 300 K is in close agreement with the expected value of  $28.34 \text{ cm}^3\text{Kmol}^{-1}$  for two uncoupled  $\text{Dy}^{\text{III}}$  ions. The  $\chi T$  product begins a slight decrease until 100 K, and then the rate of decrease becomes gradually larger. Finally, the  $\chi T$  product further decreases sharply and reaches a minimum of  $20.55 \text{ cm}^3\text{Kmol}^{-1}$  at 2 K. Thermal depopulation of the Stark sublevels is mainly responsible for the decrease. The weak antiferromagnetic interactions between the metal centers may also make some contribution.

Fitting the experimental data ranging from 50–300 K to Curie–Weiss law gives the Curie constants ( $C$ ) of 14.62, 22.24, 27.93  $\text{cm}^3\text{Kmol}^{-1}$ , 22.56 and  $28.40 \text{ cm}^3\text{Kmol}^{-1}$ , and Weiss constant ( $\theta$ ) of  $-2.71$ , 3.42, 3.15,  $-3.43$ , and  $-2.17 \text{ K}$  for **1–5**,

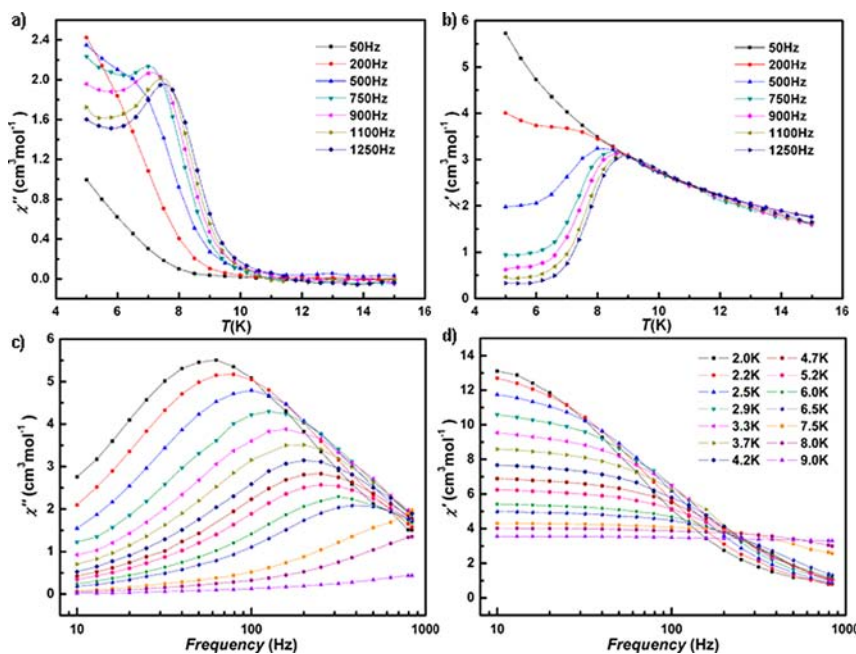


**Figure 7.** Temperature dependence of the out-of-phase (a) and in-phase (b) ac susceptibility and frequency dependence of out-of-phase (c) and in-phase (d) ac susceptibilities for compound **3** under zero dc field.

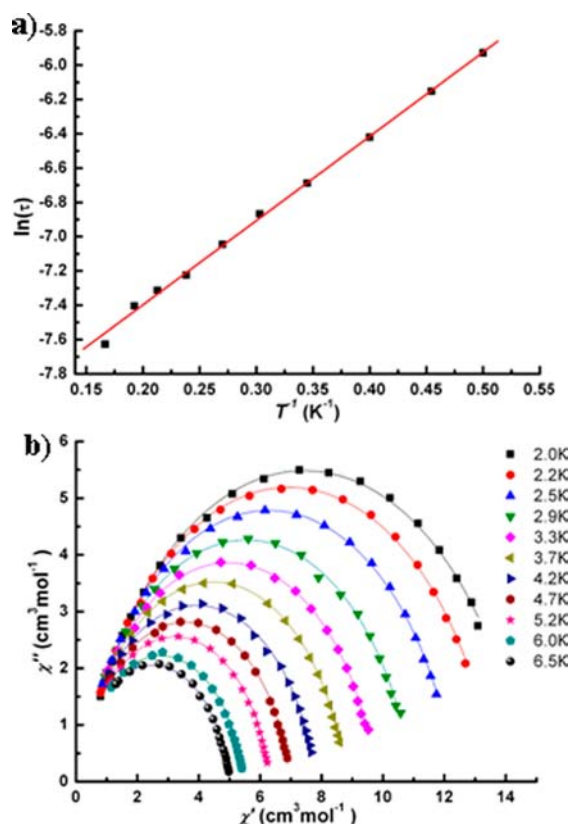


**Figure 8.** (a) Relaxation time,  $\ln(\tau)$ , versus  $T^{-1}$  plot for 3 under zero dc field. The solid line is fitted with Arrhenius law. (b) Cole–Cole plots measured in zero dc field for compound 3. The solid lines are the best fits to the experiment data. The solid line is fitted with Arrhenius law.

respectively. The small negative  $\theta$  indicates weak antiferromagnetic interactions between spin carriers in compounds 1, 4, and 5, and the small positive  $\theta$  indicates weak ferromagnetic interactions between spin carriers in compounds 2 and 3. The temperature dependence of the magnetic susceptibilities for all of the compounds shows that the magnetic behaviors may result from the match between the thermal depopulation of the Stark sublevels and magnetic interactions.<sup>12e</sup>

Field-dependence measurements of the magnetization up to 5T were performed at 2 K for compounds 1–5, as shown in Figure S2 of the Supporting Information. The values of the magnetization at 5T are 5.05, 10.50, 11.48, 10.69, and 11.69  $\mu_B$ , respectively. All of them are far lower than the expected saturation value of 10  $\mu_B$  for each  $Dy^{III}$  ion and 9  $\mu_B$  for each  $Tb^{III}$  ion. The primary reason may be spin orbit coupling, and crystal-field effect may also make some contributions.<sup>26</sup> The lack of saturation on the  $M$  vs  $H$  data confirms the presence of a significant magnetic anisotropy and/or low lying excited states. For compound 3, a narrow hysteresis loop was observed at 2.0 K. The existence of a quantum tunneling regime may explain that fact that hysteresis is not observed at higher temperature. For the same reason, the  $M$  vs  $H$  for 1 do not show hysteresis at 2.0 K (Figure S3 of the Supporting Information).

The dynamics of the magnetization were investigated using alternating-current (ac) susceptibility measurements in the zero dc field and a 3.0 G ac field. As shown in Figure 5, frequency-dependent on alternating-current magnetic susceptibilities are observed in complex 1. This indicates the presence of slow magnetic relaxation at low temperature, and thus probable SCM

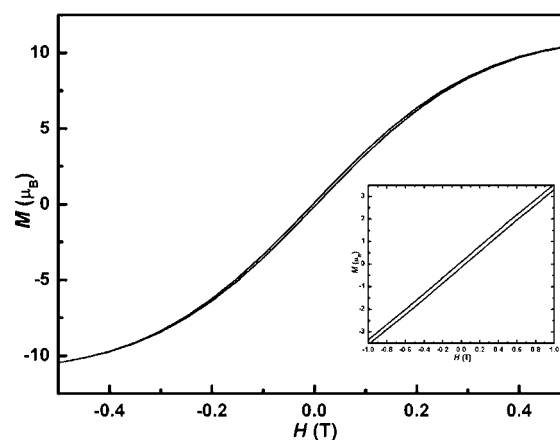


**Figure 9.** Hysteresis loops for compound 3.

behavior. The relaxation time was extracted from the frequency-dependent data between 2.0 and 3.7 K, and the Arrhenius plot obtained from these data is given in Figure 6a. The relaxation follows a thermally activated mechanism with an energy gap of 2.5 K and a pre exponential factor of  $\tau_0 = 9.98 \times 10^{-5}$  s. Cole–Cole diagrams of 1 were obtained by using the Debye functions (Figure 6b), and the curves illustrate probably the presence of a single relaxation process, as they can be fitted to the generalized Debye model  $\alpha < 0.21$ .<sup>27</sup> As shown in Figure 7, both in-phase ( $\chi'$ ) and out-of-phase ( $\chi''$ ) susceptibilities of compound 3 exhibit the frequency dependence maximum, which reveals a slow relaxation of the magnetization, and thus probable SMM behavior. The relaxation time was extracted from the frequency-dependent data between 2.0 and 6.0 K. The best fit of the experimental data to the Arrhenius equation gives an energy gap of 4.9 K and a preexponential factor of  $\tau_0 = 2.28 \times 10^{-4}$  s (Figure 8a). The data plotted as Cole–Cole plots can be fitted to the generalized Debye model with  $\alpha$  parameters below 0.18 (Figure 8b), indicating the presence of a single relaxation process. On the contrary, no out-of-phase signals were observed in compounds 2, 4, and 5.

Interestingly, the structures of  $Dy_2$  cores are very similar in complexes 3 and 5 (Figure 2 and Figure 3), but they exhibit distinct magnetic behaviors. Although it has been proven that the coordination number and coordination geometry have very important effect on the magnetic behaviors of lanthanide complexes,<sup>28,12e,14</sup> they may not play a key role this time. All of the  $Dy^{III}$  ions are eight coordinated in the two complexes, and the geometries of coordination sphere around the dysprosium ions are also similar. In compound 3 (Figure 9), the Dy–F bond distribute between 2.245(2) and 2.428(4), and the Dy–F–Dy angle is 112.39(3)°. In compound 5, the Dy–O bond distribute between 2.267(2) and 2.541(4) for Dy1 and between 2.241(4) and 2.473(4) for Dy2, and the Dy–O–Dy angles are 110.90(6)° and 113.34(9)°. All of them are insignificantly different. Thus, it may be inferred that the different magnetic behaviors are mainly caused by the presence of bridging  $F^-$  ions in compound 3. The bridging  $F^-$  ions may modify both the overlap of the magnetic orbitals of the  $Dy^{III}$  ions and the easy axes of the  $Dy^{III}$  ions, as the result of the smaller ionic radius and the larger electronegativity. The different crystal field effects, which are caused by F donors and O donors, may also make important contributions to the distinct magnetic behaviors. Therefore, both the magnetic interactions and the dynamic magnetic behaviors are evidently different between compounds 3 and 5.

## CONCLUSIONS

In summary, three fluoride-bridged lanthanide compounds **1**, **2**, and **3** have been obtained. The magnetic measurements show that the complexes **1**, **2**, and **3** exhibit intramolecular ferromagnetic interactions, while only antiferromagnetic interactions are observed in hydroxyl-bridged compounds **4** and **5**. Among these compounds, **1** and **3** show frequency-dependent ac-susceptibility indicative of slow magnetic relaxation. Because the structures of Dy<sub>2</sub> cores are very similar in compounds **3** and **5**, these significant disparities are most likely due to the differences of bridging ligands for the respective dinuclear cores. The bridging F<sup>-</sup> ions not only promote magnetic exchange interactions, but also induce slow magnetic relaxation. The successful synthesis of the three fluoride-bridged coordination compounds may open up new opportunities for the construction of SMMs based on fluoride ligand.

## ASSOCIATED CONTENT

### Supporting Information

Crystallographic details in CIF format, selected bond length Table S1, XPS (Figure S1), magnetic measurements (Figure S2–S4), XRPD patterns (Figure S5–S9). This material is available free of charge via the Internet at <http://pubs.acs.org>.

## AUTHOR INFORMATION

### Corresponding Author

\*Phone: +86-431-85168662. Fax: +86-431-85168624. E-mail: [zshi@mail.jlu.edu.cn](mailto:zshi@mail.jlu.edu.cn).

### Notes

The authors declare no competing financial interest.

## ACKNOWLEDGMENTS

This work was supported by the Foundation of the National Natural Science Foundation of China (Nos. 20971054 and 90922034), and Specialized Research Fund for the Doctoral Program of Higher Education.

## REFERENCES

- (1) (a) Caneschi, A.; Gatteschi, D.; Sessoli, R.; Barra, A. L.; Brunel, L. C.; Guillot, M. *J. Am. Chem. Soc.* **1991**, *113*, 5873–5874. (b) Sessoli, R.; Gatteschi, D.; Caneschi, A.; Novak, M. A. *Nature* **1993**, *365*, 141–143. (c) Sessoli, R.; Tsai, H. L.; Schake, A. R.; Wang, S.; Vincent, J. B.; Folting, K.; Gatteschi, D.; Christou, G.; Hendrickson, D. N. *J. Am. Chem. Soc.* **1993**, *115*, 1804–1816.
- (2) (a) Leuenberger, M. N.; Loss, D. *Nature* **2001**, *410*, 789–793. (b) Hill, S.; Edwards, R. S.; Aliaga-Alcalde, N.; Christou, G. *Science* **2003**, *302*, 1015–1018. (c) Yamanouchi, M.; Chiba, D.; Matsukura, F.; Ohno, H. *Nature* **2004**, *428*, 539–542. (d) Saitoh, E.; Miyajima, H.; Yamaoka, T.; Tataru, G. *Nature* **2004**, *432*, 203–206. (e) Bogani, L.; Wernsdorfer, W. *Nat. Mater.* **2008**, *7*, 179–186.
- (3) (a) Bagai, R.; Christou, G. *Chem. Soc. Rev.* **2009**, *38*, 1011–1026. (b) Coronado, E.; Forment-Aliaga, A.; Gaita-Arino, A.; Gimenez-Saiz, C.; Romero, F. M.; Wernsdorfer, W. *Angew. Chem., Int. Ed.* **2004**, *43*, 6152–6156. (c) Tasiopoulos, A. J.; Vinslava, A.; Wernsdorfer, W.; Abboud, K. A.; Christou, G. *Angew. Chem., Int. Ed.* **2004**, *43*, 2117–2121. (d) Ako, A. M.; Hewitt, I. J.; Mereacre, V.; Clérac, R.; Wernsdorfer, W.; Anson, C. E.; Powell, A. K. *Angew. Chem., Int. Ed.* **2006**, *45*, 4926–4929.
- (4) (a) Sorace, L.; Benelli, C.; Gatteschi, D. *Chem. Soc. Rev.* **2011**, *40*, 3092–3104. (b) Rinehart, J. D.; Long, J. R. *Chem. Sci.* **2011**, *2*, 2078–2085.
- (5) (a) Sessoli, R.; Powell, A. K. *Coord. Chem. Rev.* **2009**, *253*, 2328–2341. (b) Hewitt, I. J.; Lan, Y.; Anson, C. E.; Luzon, J.; Sessoli, R.; Powell, A. K. *Chem. Commun.* **2009**, *45*, 6765–6767.

- (6) (a) Feltham, H. L. C.; Lan, Y.; Klöwer, F.; Ungur, L.; Chibotaru, L. F.; Powell, A. K.; Brooker, S. *Chem.—Eur. J.* **2011**, *17*, 4362–4365. (b) Watanabe, A.; Yamashita, A.; Nakano, M.; Yamamura, T.; Kajiwara, T. *Chem.—Eur. J.* **2011**, *17*, 7428–7432. (c) Yang, P. P.; Gao, X. F.; Song, H. B.; Zhang, S.; Mei, X. L.; Li, L. C.; Liao, D. Z. *Inorg. Chem.* **2011**, *50*, 720–722.

- (7) (a) Tang, J.; Hewitt, I.; Madhu, N. T.; Chastanet, G.; Wernsdorfer, W.; Anson, C. E.; Benelli, C.; Sessoli, R.; Powell, A. K. *Angew. Chem., Int. Ed.* **2006**, *45*, 1729–1733. (b) Lin, P. H.; Burchell, T. J.; Ungur, L.; Chibotaru, L. F.; Wernsdorfer, W.; Murugesu, M. *Angew. Chem., Int. Ed.* **2008**, *48*, 9489–9492. (c) Hewitt, I. J.; Tang, J.; Madhu, N. T.; Anson, C. E.; Lan, Y.; Luzon, J.; Etienne, M.; Sessoli, R.; Powell, A. K. *Angew. Chem., Int. Ed.* **2010**, *49*, 6352–6356. (d) Lin, P. H.; Sun, W. B.; Yu, M. F.; Li, G. M.; Yan, P. F.; Murugesu, M. *Chem. Commun.* **2011**, *47*, 10993–10995. (e) Long, J.; Habib, F.; Lin, P. H.; Korobkov, I.; Enright, G.; Ungur, L.; Wernsdorfer, W.; Chibotaru, L. F.; Murugesu, M. *J. Am. Chem. Soc.* **2011**, *133*, 5319–5328. (f) Guo, F. S.; Liu, J. L.; Leng, J. D.; Meng, Z. S.; Lin, Z. J.; Tong, M. L.; Gao, S.; Ungur, L.; Chibotaru, L. F. *Chem.—Eur. J.* **2011**, *17*, 2458–2466.

- (8) (a) Ke, H.; Xu, G. F.; Guo, Y. N.; Gamez, P.; Beavers, C. M.; Teat, S. J.; Tang, J. *Chem. Commun.* **2010**, *46*, 6057–6059. (b) Kong, X. J.; Wu, Y.; Long, L. S.; Zheng, L. S.; Zheng, Z. *J. Am. Chem. Soc.* **2009**, *131*, 6918–6919. (c) Zheng, Y. Z.; Lan, Y.; Wernsdorfer, W.; Anson, C. E.; Powell, A. K. *Chem.—Eur. J.* **2009**, *15*, 12566–12570.

- (9) (a) Benelli, C.; Caneschi, A.; Gatteschi, D.; Pardi, L.; Rey, P. *Inorg. Chem.* **1990**, *29*, 4228–4234. (b) Bogani, L.; Sangregorio, C.; Sessoli, R.; Gatteschi, D. *Angew. Chem., Int. Ed.* **2005**, *44*, 5817–5821. (c) Bernot, K.; Luzon, J.; Caneschi, A.; Gatteschi, D.; Sessoli, R.; Bogani, L.; Vindigni, A.; Rettori, A.; Pini, M. G. *Phys. Rev. B: Condens. Matter* **2009**, *79*, 134419.

- (10) (a) Gass, I. A.; Moubaraki, B.; Langley, S. K.; Batten, S. R.; Murray, K. S. *Chem. Commun.*, **2012**, *48*, DOI: 10.1039/c2cc16946k. (b) Tian, H.; Wang, M.; Zhao, L.; Guo, Y. N.; Guo, Y.; Tang, J.; Liu, Z. *Chem.—Eur. J.* **2012**, *18*, 441–445. (c) Tian, H.; Zhao, L.; Guo, Y. N.; Guo, Y.; Tang, J.; Liu, Z. *Chem. Commun.* **2012**, *48*, 708–710.

- (11) Ma, Y.; Xu, G. F.; Yang, X.; Li, L. C.; Tang, J.; Yan, S. P.; Cheng, P.; Liao, D. Z. *Chem. Commun.* **2010**, *46*, 8264–8266.

- (12) (a) Blegg, R. J.; Muryn, C. A.; McInnes, E. J.; Tuna, F.; Winpenny, R. E. P. *Angew. Chem., Int. Ed.* **2011**, *50*, 6530–6533. (b) Guo, Y. N.; Xu, G. F.; Wernsdorfer, W.; Ungur, L.; Guo, Y.; Tang, J.; Zhang, H. J.; Chibotaru, L. F.; Powell, A. K. *J. Am. Chem. Soc.* **2011**, *133*, 11948–11951. (c) Gao, Y.; Xu, G. F.; Zhao, L.; Tang, J.; Liu, Z. *Inorg. Chem.* **2009**, *48*, 11495–11497. (d) Yang, P. P.; Gao, X. F.; Song, H. B.; Zhang, S.; Mei, X. L.; Li, L. C.; Liao, D. Z. *Inorg. Chem.* **2011**, *50*, 720–722. (e) Guo, Y. N.; Chen, X. H.; Xue, S.; Tang, J. *Inorg. Chem.* **2011**, *50*, 9705–9713.

- (13) Xu, G. F.; Wang, Q. L.; Gamez, P.; Ma, Y.; Clérac, R.; Tang, J.; Yan, S. P.; Cheng, P.; Liao, D. Z. *Chem. Commun.* **2010**, *46*, 1506–1508.

- (14) Pointillart, F.; Klementieva, S.; Kuropatov, V.; Gal, Y. L.; Stéphane, G.; Cador, O.; Cherkasov, V.; Ouahab, L. *Chem. Commun.* **2012**, *48*, 714–716.

- (15) (a) Rinehart, J. D.; Fang, M.; Evans, W. J.; Long, J. R. *Nat. Chem.* **2011**, *3*, 538–542. (b) Rinehart, J. D.; Fang, M.; Evans, W. J.; Long, J. R. *J. Am. Chem. Soc.* **2011**, *133*, 14236–14239.

- (16) Birk, T.; Magnussen, M. J.; Piligkos, S.; Weihe, H.; Holten, A.; Bendix, J. *J. Fluoride Chem.* **2010**, *131*, 898–906.

- (17) (a) Larsen, F. K.; McInnes, E. J. L.; Mkami, H. E.; Overgaard, J.; Piligkos, S.; Rajaraman, G.; Rentschler, E.; Smith, A. A.; Smith, G. M.; Boote, V.; Jennings, M.; Timco, G. A.; Winpenny, R. E. P. *Angew. Chem., Int. Ed.* **2003**, *42*, 101–105. (b) Affronte, M.; Carretta, S.; Timco, G. A.; Winpenny, R. E. P. *Chem. Commun.* **2007**, 1789–1797. (c) Meally, S. T.; Mason, K.; McArdle, P.; Brechin, E. K.; Ryder, A. G.; Jones, L. F. *Chem. Commun.* **2009**, 7024–7026. (d) Sañudo, E. C.; Faust, T. B.; Muryn, C. A.; Pritchard, R. G.; Timco, G. A.; Winpenny, R. E. P. *Inorg. Chem.* **2009**, *48*, 9811–9818. (e) Birk, T.; Pedersen, K. S.; Piligkos, S.; Thuesen, C. A.; Weihe, H.; Bendix, J. *Inorg. Chem.* **2011**, *50*, 5312–5314. (f) McRobbie, A.; Sarwar, A. R.; Yeninas, S.; Nowell, H.; Baker, M. L.; Allen, D.; Luban, M.; Muryn, C. A.

Pritchard, R. G.; Prozorov, R.; Timco, G. A.; Tuna, F.; Whitehead, G. F. S.; Winpenny, R. E. P. *Chem. Commun.* **2011**, *47*, 6251–6253.

(18) (a) Romanelli, M.; Kumar, G. A.; Emge, T. J.; Riman, R. E.; Brennan, J. G. *Angew. Chem., Int. Ed.* **2008**, *47*, 6049–6051. (b) Deacon, G. B.; Forsyth, C. M.; Junk, P. C.; Wang, J. *Chem.—Eur. J.* **2009**, *15*, 3082–3092. (c) Deacon, G. B.; Meyer, G.; Stellfeldt, D. *Eur. J. Inorg. Chem.* **2000**, 1061–1071. (d) Deacon, G. B.; Evans, D. J.; Junk, P. C.; Lork, E.; Mews, R.; Žemva, B. *Dalton Trans.* **2005**, 2237–2238.

(19) (a) Baggio, R.; Garland, T. M.; Perec, M. *Inorg. Chem.* **1997**, *36*, 950–950. (b) Aramendia, P. F.; Baggio, R.; Garland, M. T.; Perec, M. *Inorg. Chim. Acta* **2000**, *303*, 306–310. (c) Kang, J. G.; Kim, T. J.; Kang, H. J.; Kang, S. K. *J. Photochem. Photobiol. A* **2006**, *174*, 28–37. (d) Baggio, R.; Garland, T. M.; Perec, M.; Vega, D. *Inorg. Chem.* **1996**, *35*, 2396–2399. (e) Kang, J. G.; Kim, T. J.; Kang, H. J.; Park, Y.; Nah, M. K. *J. Lumin.* **2008**, *128*, 1867–1872.

(20) Sheldrick, G. M. *SADABS, the Siemens Area Detector Absorption Correction*; University of Göttingen: Göttingen, Germany, 2005.

(21) Fairhurst, S. A.; Hughes, D. L.; Leigh, G. J.; Sanders, J.; Weisner, J. *J. Chem. Soc. Dalton. Trans.* **1994**, 2591–2598.

(22) (a) Habib, F.; Lin, P.; Long, J.; Korobkov, I.; Wernsdorfer, W.; Murugesu, M. *J. Am. Chem. Soc.* **2011**, *133*, 8830–8833. (b) Pointillart, F.; Gal, Y. L.; Golhen, S.; Cador, O.; Ouahab, L. *Chem.—Eur. J.* **2011**, *17*, 10397–10404. (c) Zou, L.; Zhao, L.; Chen, P.; Guo, Y.; Guo, Y.; Li, Y.; Tang, J. *Dalton. Trans.* **2012**, *41*, 2966–2971. (d) Plass, W.; Fries, G. *Z. Anorg. Allg. Chem.* **1997**, *623*, 1205–1207.

(23) (a) Xie, Z.; Liu, Z.; Xue, F.; Mak, T. C. W. *J. Organomet. Chem.* **1997**, *539*, 127–130. (b) Xie, Z.; Chui, K.; Yang, Q.; Mak, T. C. W.; Sun, J. *Organometallics* **1998**, *17*, 3937–3944. (c) Evans, W. J.; Giarikos, G. D.; Johnston, M. A.; Greci, M. A.; Ziller, J. W. *J. Chem. Soc., Dalton. Trans.* **2002**, 520–526.

(24) Kahn, M. L.; Ballou, R.; Porcher, P.; Kahndagger, O.; Sutter, J. P. *Chem.—Eur. J.* **2002**, *8*, 525–531.

(25) Lin, P. H.; Burchell, T. J.; Clérac, R.; Murugesu, M. *Angew. Chem., Int. Ed.* **2008**, *47*, 8848–8851.

(26) Osa, S.; Kido, T.; Matsumoto, N.; Re, N.; Pochaba, A.; Mrozinski, J. *J. Am. Chem. Soc.* **2004**, *126*, 420–421.

(27) Aubin, S. M. J.; Sun, Z.; Pardi, L.; Krzystek, J.; Folting, K.; Brunel, L. C.; Rheingold, A. L.; Christou, G.; Hendrickson, D. N. *Inorg. Chem.* **1999**, *38*, 5329–5340.

(28) Ke, H.; Gamex, P.; Zhao, L.; Xu, G. F.; Xue, S.; Tang, J. *Inorg. Chem.* **2010**, *49*, 7549–7557.